

# On Modeling of Oblique Propagation of Acoustic Waves in Infinitely Long Grating Structures

無限周期構造における弾性波動斜め伝搬のモデル化  
Gongbin Tang<sup>1,2</sup>, Tao Han<sup>1</sup>, Jing Chen<sup>1</sup>, Tatsuya Omori<sup>2</sup>, and Ken-ya Hashimoto<sup>2,1†</sup>  
(<sup>1</sup>Shanghai Jiatong University, <sup>2</sup>Chiba University)  
唐 供賓<sup>1,2</sup>, 韓 韜<sup>1</sup>, 陳 景<sup>1</sup>, 大森 達也<sup>2</sup>, 橋本 研也<sup>2,1†</sup> (<sup>1</sup>上海交通大学, <sup>2</sup>千葉大学)

## 1. Summary

For designing high-performance surface acoustic wave (SAW) resonators, SAW energy must be confined well within the device structure toward not only the longitudinal ( $x$ ) but also transverse ( $y$ ) directions. Or the lateral leakage causes degradation of the resonator quality factor. However, when the wave guiding is strong, higher-order resonances may appear<sup>1,2)</sup>.

For the analysis of in-plane SAW propagation, a behavior model called the scalar potential theory<sup>3)</sup> has been widely used. It can be integrated into the coupling-of-mode (COM) theory<sup>4)</sup> and the p-matrix theory<sup>5)</sup> to take the influence of SAW excitation and reflection into account. Recently, the authors proposed another behavior model named the “thin plate model”, based on wave equations to take various complicated effects into account<sup>6)</sup>.

Full wave simulations such as the finite element analysis are quite powerful, and we can analyze SAW propagation in various structures in good accuracy. However, their computation speed is still slow, and we must use an appropriate behavior model for the simulation of practical SAW devices.

This paper discusses how parameters required in the behavior models should be extracted from results obtained by the full wave analysis.

## 2. Resonance condition

Let us consider SAW propagation in a periodic grating shown in Fig. 1. In the figure,  $p$  is the grating period. When the grating extends infinitely to both the  $x$  and  $y$  directions, the Floquet theorem indicates that the displacement field  $u$  can be expressed in the following form:

$$u = \sum_{n=-\infty}^{+\infty} U_n \exp(-j\beta_n x - j\beta_y y) \quad (1)$$

where  $U_n$  is the expansion coefficient,  $\beta_n = \beta_x + 2n\pi/p$ , and  $\beta_x$  and  $\beta_y$  are the wavenumbers of the grating mode toward the  $x$  and  $y$  directions, respectively.

In SAW devices, acoustic resonances including transversal ones occur when both  $\beta_x$  and  $\beta_y$  are real, and they can be excited efficiently by IDTs only when  $\beta_x \sim \pi/p$ . Thus we focus our efforts on analysis and modelling of variation of  $\beta_y$  with the frequency

when  $\beta_x$  is fixed at  $\pi/p$ .

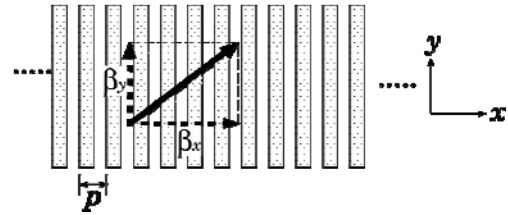


Fig. 1 SAW Propagation in infinitely long grating

## 3. Simple model

Here we discuss wave propagation in the structure shown in Fig. 1 by the use of thin plate model<sup>6)</sup>, but electrical excitation is ignored. In the model, stiffness  $c_{ij}$  is assumed to be uniform throughout the structure, and variation of the structure is considered as that of the mass density  $\rho$ .

Let us consider propagation of shear vertical waves in the  $x$ - $y$  plane. Then its propagation is governed by the following wave equation:

$$\frac{\partial^2 u}{\partial x^2} + \gamma \frac{\partial^2 u}{\partial y^2} + \frac{\rho(x)\omega^2}{c_{55}} u = 0 \quad (2)$$

where  $c_{ij}$  is the stiffness,  $\omega$  is the radial frequency, and  $\gamma = c_{44}/c_{55}$  is a parameter of the substrate anisotropy. Since  $\rho$  changes periodically with  $x$ , it is expressed in the Fourier Expansion form as

$$\rho(x) = c_{55} \sum_{n=-\infty}^{+\infty} R_n \exp(-2n\pi j x / p) \quad (3)$$

where  $R_n$  is the expansion coefficient. Note that  $R_{-n} = R_n^*$  because  $\rho(x)$  is real, and  $R_n$  is real when the structure is symmetric with respect to the  $x_2$  axis.

Substitution of Eqs. (1) and (3) into (2) gives

$$\sum_{n=-\infty}^{+\infty} \left\{ -\beta_n^2 U_n - \gamma \beta_y^2 U_n + \omega^2 \sum_{m=-\infty}^{+\infty} R_{m-n} U_m \right\} \times \exp(-j\beta_n x - j\beta_y y) = 0 \quad (4)$$

So that Eq.(4) holds for arbitrary  $x$ , the following condition must be satisfied for arbitrary  $n$ :

$$-\beta_n^2 U_n(y) - \gamma \beta_y^2 U_n + \omega^2 \sum_{m=-\infty}^{+\infty} R_{m-n} U_m(y) = 0 \quad (5)$$

When we consider only the coupling between the components with  $n=0$  and  $n=1$ , Eq. (5) reduces to

$$\left( \beta_0^2 + \gamma \beta_y^2 - \omega^2 R_0 \right) \left( \beta_{-1}^2 + \gamma \beta_y^2 - \omega^2 R_0 \right) - \omega^4 |R_1|^2 = 0 \quad (6)$$

†k.hashimoto@ieee.org

Fig. 2 shows the calculated  $\beta_x$ - $\beta_y$  curve at  $\omega p R^{0.5} = \pi/2$ . In the calculation,  $\gamma$  is set at unity (isotropic), and  $|R_1|$  is set at  $0.0475\pi/p$ .

Two semi-circles centered at  $\beta_x=0$  and  $\beta_x=2\pi/p$  are seen. The former corresponds to the forward propagating mode, and the latter does a component of the backward propagating mode generated by the spatial modulation in the periodic grating.

Two imaginary branches start from the edges of semi-circles where  $\beta_y=0$ . They correspond to the evanescent modes (decaying toward the  $\pm y$  direction).

When  $\beta_x = \pi/p$ , Eq. (6) reduces to 
$$\beta_y^2 = \gamma^{-1} [\omega^2 (R_0 \pm |R_1|) - (\pi/p)^2]. \quad (7)$$

When  $\omega p / \pi < (R_0 \pm |R_1|)^{0.5}$ ,  $\beta_y$  is imaginary, namely, evanescent toward the  $x$  direction, and thus the transverse mode resonance does not occur in this frequency region. On the other hand, when  $\omega p / \pi > (R_0 \pm |R_1|)^{0.5}$ ,  $\beta_y$  is real. Thus transverse mode resonances will occur provided that the transverse resonance condition is also satisfied.

In Eq. (7), the plus sign specifies the branch passing through the lower stopband edge while the minus sign specifies the branch passing through the upper stopband edge.

It should be noted that, when the IDT structure is symmetric with respect to the  $y$  axis, i.e., when  $R_n$  is pure real, one of these two branches are electrically excitable. Namely, the branch with the plus sign is electrically excitable when the main resonance occurs close to the lower stopband edge while the branch with the minus sign is excitable when the main resonance occurs close to the upper stopband edge. The remaining branch will be also excited when the resonator structure possesses asymmetry.

We can also derive Eq. (7) from the two dimensional COM theory<sup>4)</sup>.

#### 4. Fitting

Fig. 3 shows variation of  $\beta_y$  with  $\omega p / V_B$  for the short-circuited Al grating with the thickness of  $0.1p$  on the  $128^\circ\text{YX-LiNbO}_3$  substrate when  $\beta_x = \pi/p$ . Here  $V_B (=4,025 \text{ m/s})$  is the slow shear bulk wave velocity. The calculation was performed by the modified version of the software OBLIQ<sup>8)</sup>, which

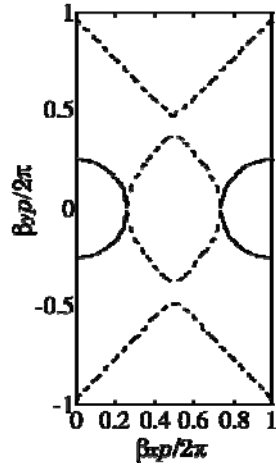


Fig. 2 Calculated  $\beta_x$ - $\beta_y$  curve at  $\omega p R^{0.5} = \pi/2$ . Solid lines: real part, and broken lines: imaginary part.

was developed by the authors to analyze SAW oblique propagation in periodic grating structures.

As we expected, when  $f < 0.498V_B/p$ ,  $\beta_y$  is imaginary, namely, evanescent toward the  $x$  direction, and when  $f > 0.498V_B/p$ ,  $\beta_y$  is real. It should be noted that  $0.498V_B/p$  corresponds to the upper edge of the stopband. Another branch of  $\beta_y$  is not shown in this figure because it is not piezoelectrically active. The branch passes through the lower edge of the stopband at  $f = 0.475V_B/p$ .

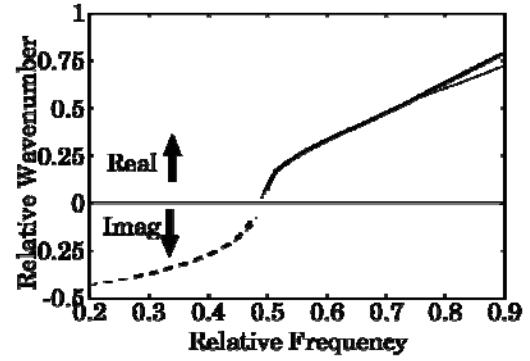


Fig. 3 Change of  $\beta_y$  with frequency when  $\beta_x = \pi/p$ . Bold lines: calculated by modified OBLIQ, and thin lines: calculated by the simple model.

In the figure,  $\beta_y$  calculated by Eq. (7) is also given. It is seen that variation of  $\beta_y$  with  $\omega$  can be modeled well by this simple model which takes the Bragg reflection into account. Discrepancy can be seen at frequencies much larger than  $0.498V_B/p$ . This may be due to complex anisotropy of the SAW slowness curve on the  $128^\circ\text{YX-LiNbO}_3$  substrate.

**Acknowledgement** The work was supported by the Natural Science Foundation of China (No.11174205, No.11474203, and No. 11404209) and the Ministry of Education of China (NCET-12-0357 and RFDP-20120073110021).

#### References

1. E.J.Steple and R.C.Smythe, Proc. IEEE Ultrason. Symp. (1975) p. 307
2. R.V.Schmidt and L.A.Coldren, Proc. IEEE Ultrason. Symp. (1975) p. 115
3. K. Hashimoto, "5.2.2 Transverse-Mode Analysis," in Surface Acoustic Wave Devices in Telecommunications (Springer, 2000) pp.131-137.
4. K.Hirota and K.Nakamura, Proc. IEEE Ultrason. Symp. (2001) p. 115
5. M.Solal, IEEE Trans. Ultrason., Ferroelect., Freq. Contr., **51**, 12 (2004) p. 1690
6. G.B.Tang, B.F.Zheng, T.Han, J.Chen, T.Omori, and K.Hashimoto, to be presented at this Symposium
7. M.Mayer, A.Bergmann, G.Kovacs, and K.Wagner, IEEE Ultrason. Symp. (2008) p. 803.
8. K.Hashimoto, G.Endoh, M.Ohmaru and M.Yamaguchi, Jpn. J. Appl. Phys., **35**, Part 1, 5B (1996) p. 3006.